

The bliss of dimensionality: how an unsupervised criterion identifies optimal low-resolution representations of high-dimensional datasets

Margherita Mele,^{1,2} Daniel Campos Moreno,³ and Raffaello Potestio^{1,2,*}

¹*Physics Department, University of Trento, via Sommarive, 14 I-38123 Trento, Italy*

²*INFN-TIFPA, Trento Institute for Fundamental Physics and Applications, I-38123 Trento, Italy*

³*Grup de Física Estadística, Departament de Física, Facultat de Ciències, Universitat Autònoma de Barcelona, 08193 Bellaterra, Barcelona, Spain*

(Dated: March 6, 2026)

Selecting the optimal resolution for discretizing high-dimensional data is a central problem in physics and data analysis, particularly in unsupervised settings where the underlying distribution is unknown. The Relevance–Resolution (Res–Rel) framework addresses this issue through an information-theoretic trade-off between descriptive detail and statistical reliability. Here we provide a systematic validation of this approach by comparing its characteristic optima–maximum relevance and the -1 slope (information-theoretic) point—with the discretization that minimizes the Kullback–Leibler divergence from a known or physically motivated ground truth distribution. Across unstructured and structured synthetic datasets, Gaussian clones of MNIST, and molecular dynamics simulations of the alanine dipeptide, we find that as the dimensionality or informative content increases the KL-optimal discretization consistently lies within the Res–Rel optimality region. Furthermore, in high-dimensional regimes the -1 slope criterion closely matches the KL divergence minimum. These results establish the quantitative consistency of unsupervised information-theoretic selection with distribution-based optimality.

Introduction — Discrete representations of continuous data cover a wide range of situations, from building simple one-dimensional histograms to complex clustering techniques for high-dimensional datasets. Such methods are ubiquitous across physics [1], data science [2], and machine learning [3], and provide the bedrock for tasks such as coarse-graining [4], density estimation [5], and model inference [6]. Here, as in many other related contexts, choosing the appropriate level of detail of the representation remains a fundamental open problem [7, 8]: indeed, overly coarse descriptions discard important structure, whereas excessively fine ones introduce sampling noise and statistical unreliability [9, 10]. This trade-off is particularly acute in finite-sample regimes and high-dimensional systems, where empirical frequencies may poorly approximate the underlying generative process of the data [11–13]. Standard criteria developed to select an adequate level of detail of the data representation often rely on supervised information about the target distribution (e.g., likelihood optimisation or divergence minimisation) [14–16], but such an approach is naturally excluded in unsupervised settings. Consequently, intrinsically data-driven criteria are needed to identify informative representations without explicit knowledge of the true probability distribution [17–19]. The Relevance–Resolution (Res–Rel) framework [20, 21] addresses this problem by introducing an information-theoretic criterion that balances representational granularity (resolution) against statistical significance (relevance). In this approach, clusters of instances of a dataset are grouped together according to a given criterion, thereby inducing a spectrum of reduced representations of the data

that are evaluated in terms of their resolution and relevance; by analysing how empirical frequency statistics changes with the number of discrete states, the framework identifies optimal resolution regimes directly from the data, without external supervision [22]. The simplicity and the unsupervised character of the framework make it extremely attractive and potentially powerful, and its increasingly numerous applications provide concrete support to its effectiveness [23–29]; furthermore, an important body of work has been done to lay solid mathematical and statistical foundations to the approach [30–33]. However, a simple, bottom-up validation of its working and its range of validity is still missing. In this letter, we addressed this problem by analysing synthetic data points generated from distributions known *a priori*, as well as realistic datasets such as MNIST and molecular dynamics trajectories of the alanine dipeptide, systematically evaluating the capability of the resolution-relevance approach to provide physically informative low-resolution representations of high-dimensional data and setting boundaries for its applicability.

Theoretical background — Consider a N -dimensional dataset of size P partitioned into n discrete states, or clusters, by a mapping that assigns each data point to a state. Let k_i denote the number of data points assigned to state i , and m_k the number of states with occupancy exactly equal to k . Resolution and relevance are defined, respectively, as:

$$H_{\text{res}} = - \sum_{i=1}^N \frac{k_i}{P} \log \frac{k_i}{P}, \quad H_{\text{rel}} = - \sum_k \frac{k m_k}{P} \log \frac{k m_k}{P}. \quad (1)$$

Resolution, H_{res} , is the Shannon entropy of the empirical distribution of frequencies, and quantifies the level of detail of the representation. Relevance, H_{rel} , in-

* raffaello.potestio@unitn.it

stead captures the heterogeneity of empirical frequencies through the occupancy distribution m_k , and so reflects the amount of statistically significant information entailed in the coarse representation of the data [22, 23]. By varying the number of states one can generate the *Relevance–Resolution* curve, which shows and quantifies the trade-off between descriptive detail and statistical reliability [30]. Resolution increases with the number of states, while relevance displays a non-monotonic behaviour: it first increases as more and more informative structure is resolved, then decreases when further refinement produces poorly sampled states dominated by noise. An optimal representation thus lies in the intermediate regime, between the maximum relevance and the point where the curve attains slope -1 , which marks the information-theoretical (IT) optimum [21, 33]. We consider this interval comprised between the relevance maximum and the IT optimum to represent the *optimality region*: beyond this point, information gains from increasing resolution are lower than the corresponding information losses by reducing statistical significance.

Each representation induces an empirical probability distribution: given a partition $\{C_j\}_{j=1}^n$ with occupancies $k_j = |C_j|$, the empirical probability assigned to each data point is $\hat{p}(x_i) = k_j/P$, for $x_i \in C_j$. If the true generative distribution $p(x)$ were known, a representation at the optimal level of resolution would minimise the discrepancy between $p(x)$ and the empirical distribution $\hat{p}(x)$. A natural measure for this is the Kullback–Leibler (KL) divergence between both distributions,

$$D_{\text{KL}}(p||\hat{p}) = \sum_i p(x_i) \log \frac{p(x_i)}{\hat{p}(x_i)}. \quad (2)$$

When evaluating the KL divergence, the reference probability density is evaluated at the data points and normalised over the dataset; the empirical representation is treated consistently, so that both induced discrete distributions are properly normalised, such that $\sum_i p(x_i) = \sum_i \hat{p}(x_i) = 1$. In typical unsupervised settings, however, the true distribution $p(x)$ is unknown and cannot be used to guide the choice of representation. The problem therefore reduces to identifying informative discretizations directly from empirical frequency statistics, and the Relevance–Resolution framework provides a fully data-driven criterion to select such representations. To assess how the representations selected by this criterion relate to optimal ones reproducing the empirical distribution, we analyse datasets for which such empirical is available—either known by construction (synthetic data) or physically/statistically motivated (real systems). This controlled setting enables a direct comparison between the Res–Rel optima and the discretisation that minimises the KL divergence from the reference. The datasets analysed and the associated analysis procedure are summarised below, with full technical details reported in the Supplementary Information (SI).

Methodology —For each dataset realisation, representations are constructed by partitioning the data into n

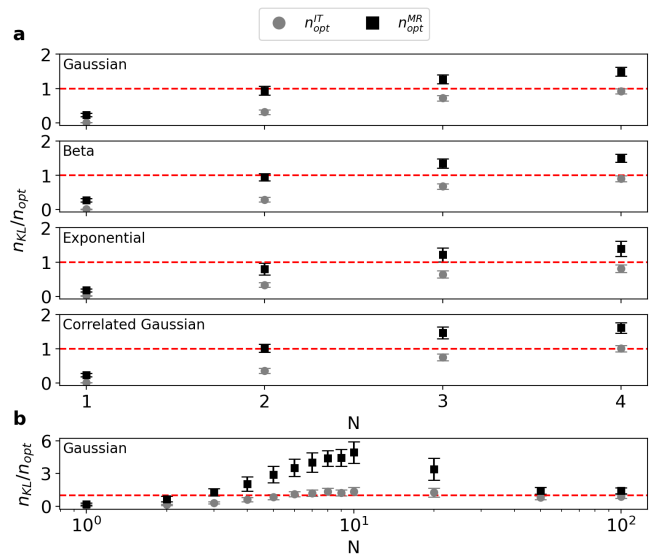


FIG. 1. **Comparison between Relevance–Resolution and Kullback–Leibler optimal representations for unstructured synthetic data.** Ratio $n_{\text{KL}}/n_{\text{opt}}$ as a function of the data dimensionality N for unstructured synthetic datasets. In each panel, black squares correspond to $n_{\text{opt}}^{\text{MR}}$ (maximum relevance), while grey circles correspond to $n_{\text{opt}}^{\text{IT}}$ (-1 slope point). The red dashed line indicates equality between the two estimates. Error bars represent the standard deviation over 50 independent realisations. Panel (a) shows low-dimensional datasets analysed using N -dimensional histograms, generated from Gaussian, Beta, Exponential, and correlated Gaussian distributions. Panel (b) shows the corresponding analysis for IID Gaussian data spanning from low to high dimensions, where representations are constructed using UPGMA clustering.

discrete states. For a first test on low-dimensional ($N \leq 4$) datasets we discretised the data space of all four distributions under examination using N -dimensional histograms; we then focussed on the case of Gaussian distributions in spaces of dimension 1 to 100, partitioning them by agglomerative clustering with UPGMA linkage [34]. The number of states n parametrises the representation and generates a unique Relevance–Resolution curve for each realisation. For every n we compute $(H_{\text{res}}, H_{\text{rel}})$, and the empirical distribution induced by the partition. From each Relevance–Resolution curve we identify two characteristic values of n : the point of maximum relevance (MR), defining $n_{\text{opt}}^{\text{MR}}$, and the point where the curve attains slope -1 , defining $n_{\text{opt}}^{\text{IT}}$. Independently, the KL divergence between the reference distribution and the empirical distribution is evaluated as a function of n , and the minimiser n_{KL} is identified. For synthetic and semi-real datasets, results are averaged over 50 independent realisations; for the alanine dipeptide [35] the analysis is performed over 10 independent MD trajectories. Implementation details and additional robustness analyses are reported in the SI.

Unstructured Synthetic Data — To establish a base-

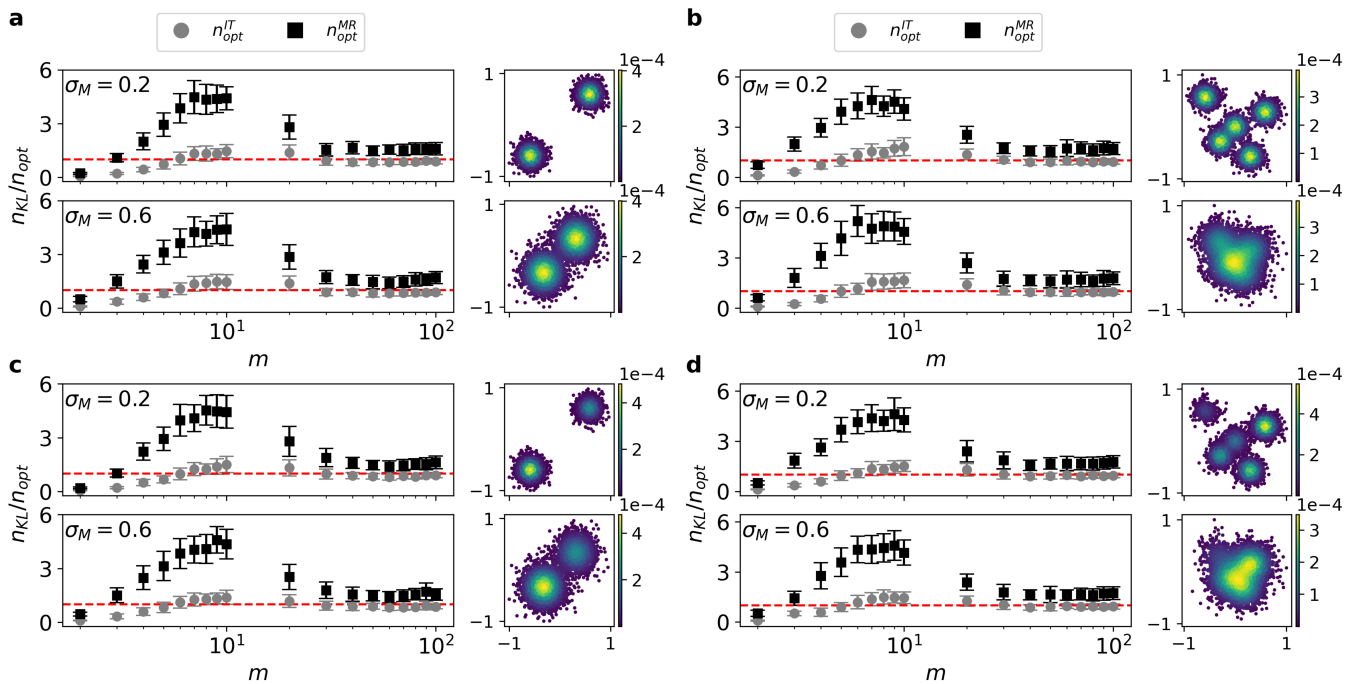


FIG. 2. **Comparison between Relevance-Resolution and Kullback-Leibler optimal representations for structured synthetic data.** Ratio $n_{\text{KL}}/n_{\text{opt}}$ as a function of the number of informative dimensions m for structured synthetic datasets with latent Gaussian mixture structure. In each panel, black squares correspond to $n_{\text{opt}}^{\text{MR}}$ (maximum relevance), while grey circles correspond to $n_{\text{opt}}^{\text{IT}}$ (-1 slope point). The red dashed line indicates equality between the two estimates. Error bars represent the standard deviation over 50 independent realisations. Panels (a) and (b) show equal-weight mixtures for $K = 2$ and $K = 5$, while panels (c,d) show the corresponding unequal-weight cases with weights $[0.66, 0.33]$ and $[0.34, 0.27, 0.19, 0.13, 0.07]$, respectively. Different rows correspond to increasing values of the mixture standard deviation σ_M , as indicated. For each row, the right-hand subpanels show two-dimensional projections of representative datasets generated with $m = 2$ for the corresponding parameter values. For each value of K , the random seed used to generate the data is fixed across different scenarios, ensuring that the relative positions of the mixture means are identical.

line, we first consider synthetic datasets without latent discrete structure, where all components are sampled independently from a prescribed continuous distribution; this setting allows us to isolate purely dimensional effects. Datasets are generated from Gaussian, beta, exponential, and correlated Gaussian distributions (see SI for technical details). For low-dimensional data ($N \leq 4$), representations are constructed *via* N -dimensional histograms, which provide a direct and controlled discretisation of the data space and constitute the natural benchmark for estimating empirical probability densities. However, the number of bins grows exponentially with N , leading to severe sparsity and unstable frequency estimates at fixed sample size [11]. To probe higher-dimensional regimes, we therefore adopt agglomerative clustering (UPGMA), which defines discrete states directly from inter-point distances without relying on a regular grid. For each dimensionality N , we compare $n_{\text{opt}}^{\text{MR}}$ and $n_{\text{opt}}^{\text{IT}}$ with the KL-optimal value n_{KL} . FIG. 1.a shows that in one dimension the Res-Rel framework overestimates the KL-optimal number of states, with both criteria yielding $n_{\text{opt}} > n_{\text{KL}}$. The discrepancy rapidly decreases with increasing N : already for $N = 2$, $n_{\text{opt}}^{\text{MR}}$ is close to n_{KL} , and for $N \geq 2$ the

KL-optimal value systematically falls within the Res-Rel optimality region defined by $[n_{\text{opt}}^{\text{MR}}, n_{\text{opt}}^{\text{IT}}]$. This behaviour is robust across all tested distributions. The analysis is extended to higher dimensions using *iid* Gaussian data (FIG. 1.b). Also in this case, the low-dimensional overestimation progressively vanishes as N increases. For intermediate dimensions the Res-Rel optimality region broadens, while for $N > 10$ the two criteria converge, yielding close values of n_{opt} . Overall, the discrepancy observed at low dimensionality progressively reduces as N increases, and the KL-optimal value falls within the Res-Rel optimality region for $N \geq 2$.

Structured Synthetic Data — Having characterised the dependence of the sheer dimensionality of the data, we now introduce latent discrete structure embedded in a high-dimensional space. The total number of dimensions is fixed to $N = 100$, of which only $m \leq N$ components carry informative signal. In the informative subspace, samples are drawn from mixtures of K Gaussian components with standard deviation σ_M , whereas the remaining dimensions consist of independent Gaussian noise with $\sigma \ll \sigma_M$ (see SI for full construction details). Both binary ($K = 2$) and multi-component ($K = 5$) mixtures,

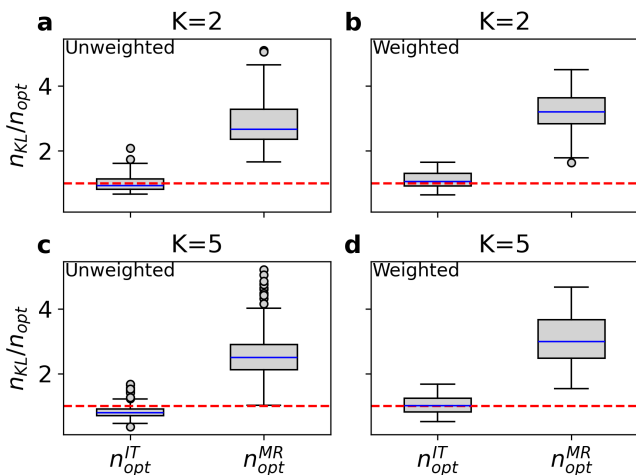


FIG. 3. **Comparison between Relevance-Resolution and Kullback-Leibler optimal representations for Gaussian clones of MNIST.** Boxplots show the ratio $n_{\text{KL}}/n_{\text{opt}}$ evaluated at two characteristic points of the Relevance-Resolution curve: the -1 -slope point $n_{\text{opt}}^{\text{IT}}$ (information-theoretic optimum) and the maximum-relevance point $n_{\text{opt}}^{\text{MR}}$. The horizontal red dashed line marks the ideal value $n_{\text{KL}}/n_{\text{opt}} = 1$, corresponding to perfect agreement between the two criteria, while blue horizontal lines indicate the median of each distribution. Panels (a,b) correspond to mixtures with $K = 2$ components, with equal weights in (a) and unequal weights $[0.66, 0.33]$ in (b). Panels (c,d) show mixtures with $K = 5$ components, with equal weights in (c) and unequal weights $[0.34, 0.27, 0.19, 0.13, 0.07]$ in (d).

with equal and unequal weights, are analysed. FIG. 2 reports the ratio between the KL-optimal number of discrete elements n_{KL} and the Res-Rel optima as a function of the number of informative dimensions m . For very low informative dimensionality ($m = 2$), the Res-Rel criteria select values exceeding n_{KL} , consistent with the behaviour observed in low-dimensional unstructured data. As m increases, the agreement improves: the KL-optimal value systematically falls within the Res-Rel optimality region and is typically located close to the -1 slope point. The width of the optimality region initially increases with m and subsequently decreases for $m \geq 10$, as the informative signal dominates the noisy background. These trends are robust across all investigated mixture configurations and signal widths (additional parameter combinations are reported in SI).

Semi-real Data: Gaussian Clones of MNIST — To bridge fully synthetic models and real-world data, we analyse Gaussian clones derived from the MNIST handwritten digit database [36]. For each selected digit class, a class-conditional multivariate Gaussian distribution is estimated from the original data and used to generate synthetic samples (“Gaussian clones”). The reference distribution is thus a Gaussian mixture with K components corresponding to distinct digit classes (see SI for estimation details). Digit 1 is excluded due to

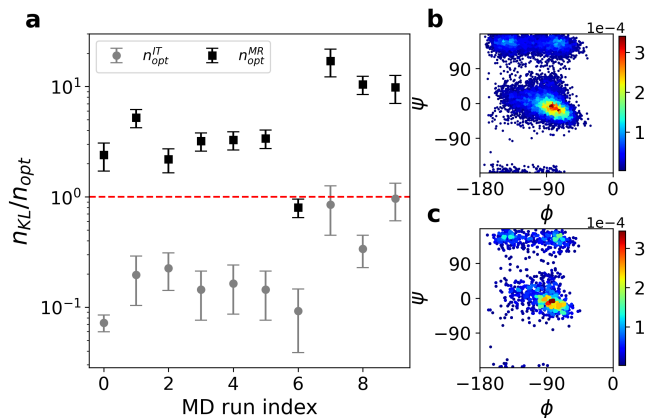


FIG. 4. **Comparison between Relevance-Resolution and Kullback-Leibler optimal representations for Alanine dipeptide.** (a) Ratio $n_{\text{KL}}/n_{\text{opt}}$ computed over ten independent molecular dynamics (MD) simulations. Grey circles denote the ratio evaluated at the maximum-relevance point $n_{\text{opt}}^{\text{MR}}$, while black squares correspond to the information-theoretic optimum $n_{\text{opt}}^{\text{IT}}$, defined as the -1 -slope point of the Relevance-Resolution curve. The horizontal red dashed line marks the reference value $n_{\text{KL}}/n_{\text{opt}} = 1$, corresponding to perfect agreement between the Kullback-Leibler-optimal discretization and the Relevance-Resolution prediction. (b,c) Two-dimensional projections in the space of backbone dihedral angles (ϕ, ψ) for a representative trajectory. In panel (b), colors represent a two-dimensional histogram of the raw MD frames, providing an empirical estimate of the reference probability distribution. In panel (c), only the centroids of the clusters obtained by RMSD-based clustering at $n_{\text{opt}}^{\text{IT}}$ are shown. Colours are assigned from a two-dimensional histogram in (ϕ, ψ) constructed over these centroids, each weighted by the multiplicity of its corresponding cluster.

its anomalous Res-Rel behaviour (see SI). We analyse mixtures with $K = 2$ and $K = 5$, considering both equal and unequal class weights. For each configuration, all possible combinations of K digit classes are examined. FIG. 3 reports the ratio $n_{\text{KL}}/n_{\text{opt}}$ evaluated at the two Res-Rel characteristic points. Across all scenarios, the -1 slope criterion yields values closely aligned with the KL-minimising discretisation, with distributions centred around $n_{\text{KL}}/n_{\text{opt}}^{\text{IT}} \simeq 1$. In contrast, the maximum-relevance criterion systematically selects smaller numbers of discrete elements, resulting in $n_{\text{KL}}/n_{\text{opt}}^{\text{MR}} > 1$, albeit with deviations remaining within a factor smaller than four. The same qualitative behaviour is observed for both equal and unequal weight mixtures and across different class combinations.

Real Data: Alanine Dipeptide — We finally consider a dataset consisting of molecular dynamics (MD) simulations of the alanine dipeptide, a standard benchmark system whose equilibrium behaviour is well described in terms of the backbone dihedral angles (ϕ, ψ) [35, 37]. As commonly done, the reference probability distribution is defined in this reduced space and estimated from each trajectory *via* a two-dimensional histogram of the dihe-

dral angles (see SI for simulation details). Discrete representations are instead constructed by clustering molecular configurations in the full configurational space using the atom-wise root mean square distance (RMSD) as a metric. This setup allows us to test whether the Res–Rel-selected discretisations recover the physically relevant probability landscape defined in dihedral angle space. FIG. 4.a reports, for ten independent trajectories, the ratio between the KL-optimal number of clusters n_{KL} and the Res–Rel optima. In all cases, n_{KL} lies within the optimality region. However, unlike the synthetic and semi-real datasets, no single Res–Rel criterion systematically coincides with the KL minimum across trajectories. FIG. 4.b-c compare, for a representative trajectory, the empirical dihedral angle density and the probability distribution reconstructed from clustering at $n_{\text{opt}}^{\text{IT}}$. The two representations display consistent large-scale conformational features. Despite the absence of an exact generative distribution and the finite-sampling nature of the reference estimate, the Res–Rel framework restricts the optimal discretisation to a narrow range of cluster numbers across independent trajectories, with a dispersion in line with what was observed in the previously discussed cases for a low number of informative features.

Concluding remarks — The systematic investigation of low-resolution representations of synthetic, semi-real, and real datasets allowed us to perform a systematic comparison between clusterings obtained from the Resolution–Relevance framework and those minimising the KL divergence from the underlying generative model. In low-dimensional regimes, the Res–Rel criteria tend to overestimate the KL minimum; as the effective dimensionality or informative content of the data increases, however, the KL-optimal number of discrete elements falls within the Res–Rel optimality region. In structured and high-dimensional settings, the -1 slope criterion provides the closest agreement with the divergence minimum. Crucially, this consistency extends to the real molecular system, where the reference distribution is empirically estimated. The Res–Rel framework therefore offers a principled, fully data-driven mechanism for selecting informative representations without requiring explicit knowledge of the underlying generative distribution. Taken together, this investigation shows that the Res–Rel criterion identifies discretisations that are statistically robust and probabilistically meaningful, effectively linking unsupervised information-theoretic selection to supervised distribution-based optimality.

I. ACKNOWLEDGEMENTS

RP acknowledges support from ICSC - Centro Nazionale di Ricerca in HPC, Big Data and Quantum Computing, funded by the European Union under NextGenerationEU. Views and opinions expressed are however those of the author(s) only and do not necessarily reflect those of the European Union or The European Research Executive Agency. Neither the European Union nor the granting authority can be held responsible for them.

This work was conducted in the spirit of the Slow Science Manifesto, advocating for collaborative and sustainable research (slow-science.com).

II. AUTHOR CONTRIBUTIONS

All authors conceived the study and proposed the method. MM produced the data and performed the analysis. RP and MM interpreted the results. All authors drafted the paper, reviewed the results, and approved the final version of the manuscript.

III. SUPPORTING INFORMATION

The Supplementary Information provides methodological details and additional analyses supporting the main text, including the definitions of relevance and resolution, and the description of the numerical procedure used to extract the optimal representation sizes, the construction of empirical and reference probabilities, the evaluation of $D_{\text{KL}}(p||\hat{p})$, the protocols used to build discrete representations (histograms and UPGMA clustering), and complete dataset specifications. It also reports supplementary results and diagnostics for the MNIST digit “1”, alanine-dipeptide visualisation, robustness and implementation checks, additional structured-synthetic parameter combinations, and KL-based analyses.

IV. DATA AVAILABILITY

The raw data associated with this work are freely available on Zenodo at <https://doi.org/10.5281/zenodo.18860257>.

-
- [1] L. P. Kadanoff, “Scaling laws for ising models near t_c ,” *Physics Physique Fizika*, vol. 2, p. 263, 1966.
 - [2] A. K. Jain, M. N. Murty, and P. J. Flynn, “Data clustering: A review,” *ACM Computing Surveys*, vol. 31, pp. 264–323, 1999.
 - [3] V. N. Vapnik, *Statistical Learning Theory*. New York: Wiley, 1998.
 - [4] K. G. Wilson and J. Kogut, “The renormalization group and the ϵ expansion,” *Physics Reports*, vol. 12, pp. 75–199, 1974.
 - [5] B. W. Silverman, *Density Estimation for Statistics and Data Analysis*. London: Routledge, 2018.
 - [6] H. Akaike, “A new look at the statistical model identification,” *IEEE Transactions on Automatic Control*, vol. 19,

- pp. 716–723, 1974.
- [7] J. Rissanen, “Modeling by shortest data description,” *Automatica*, vol. 14, pp. 465–471, 1978.
 - [8] V. N. Vapnik and A. Y. Chervonenkis, “On the uniform convergence of relative frequencies of events to their probabilities,” in *Measures of Complexity: Festschrift for Alexey Chervonenkis*, pp. 11–30, Cham: Springer, 2015.
 - [9] P. J. Bickel and E. Levina, “Some theory for fisher’s linear discriminant function, naive bayes, and some alternatives when there are many more variables than observations,” *Bernoulli*, vol. 10, pp. 989–1010, 2004.
 - [10] M. J. Wainwright, *High-Dimensional Statistics: A Non-Asymptotic Viewpoint*. Cambridge: Cambridge University Press, 2019.
 - [11] R. Bellman, “Dynamic programming,” *Science*, vol. 153, pp. 34–37, 1966.
 - [12] L. Devroye, L. Györfi, and G. Lugosi, *A Probabilistic Theory of Pattern Recognition*. New York: Springer, 2013.
 - [13] M. Belkin, D. Hsu, S. Ma, and S. Mandal, “Reconciling modern machine-learning practice and the classical bias–variance trade-off,” *Proceedings of the National Academy of Sciences*, vol. 116, pp. 15849–15854, 2019.
 - [14] A. Gelman, J. Hwang, and A. Vehtari, “Understanding predictive information criteria for bayesian models,” *Statistics and Computing*, vol. 24, pp. 997–1016, 2014.
 - [15] G. Schwarz, “Estimating the dimension of a model,” *The Annals of Statistics*, vol. 6, pp. 461–464, 1978.
 - [16] K. P. Burnham and D. R. Anderson, *Model Selection and Multimodel Inference: A Practical Information-Theoretic Approach*. New York: Springer, 2 ed., 2004.
 - [17] N. Tishby and N. Zaslavsky, “Deep learning and the information bottleneck principle,” in *2015 IEEE Information Theory Workshop (ITW)*, (Jerusalem), pp. 1–5, IEEE, 2015.
 - [18] A. Jaiswal, A. R. Babu, M. Z. Zadeh, D. Banerjee, and F. Makedon, “A survey on contrastive self-supervised learning,” *Technologies*, vol. 9, p. 2, 2021.
 - [19] Y. LeCun, Y. Bengio, and G. Hinton, “Deep learning,” *Nature*, vol. 521, pp. 436–444, 2015.
 - [20] M. Marsili, I. Mastromatteo, and Y. Roudi, “On sampling and modeling complex systems,” *Journal of Statistical Mechanics: Theory and Experiment*, vol. 2013, p. P09003, 2013.
 - [21] A. Haimovici and M. Marsili, “Criticality of mostly informative samples: A bayesian model selection approach,” *Journal of Statistical Mechanics: Theory and Experiment*, vol. 2015, p. P10013, 2015.
 - [22] M. Marsili and Y. Roudi, “Quantifying relevance in learning and inference,” *Physics Reports*, vol. 963, pp. 1–43, 2022.
 - [23] S. Grigolon, S. Franz, and M. Marsili, “Identifying relevant positions in proteins by critical variable selection,” *Molecular BioSystems*, vol. 12, pp. 2147–2158, 2016.
 - [24] C. Battistin, B. Dunn, and Y. Roudi, “Learning with unknowns: Analyzing biological data in the presence of hidden variables,” *Current Opinion in Systems Biology*, vol. 1, pp. 122–128, 2017.
 - [25] R. Holtzman, M. Giulini, and R. Potestio, “Making sense of complex systems through resolution, relevance, and mapping entropy,” *Physical Review E*, vol. 106, p. 044101, 2022.
 - [26] M. Mele, R. Covino, and R. Potestio, “Information-theoretical measures identify accurate low-resolution representations of protein configurational space,” *Soft Matter*, vol. 18, pp. 7064–7074, 2022.
 - [27] J. Morand, S. Yip, Y. Velegrakis, G. Lattanzi, R. Potestio, and L. Tubiana, “Quality assessment and community detection methods for anonymized mobility data in the italian covid context,” *Scientific Reports*, vol. 14, p. 4636, 2024.
 - [28] R. Aldrigo, R. Menichetti, and R. Potestio, “Low-resolution descriptions of model neural activity reveal hidden features and underlying system properties,” *Physical Review E*, vol. 111, p. 044315, 2025.
 - [29] M. Mele, R. Fiorentini, T. Tarenzi, G. Mattiotti, and R. Potestio, “Determining the optimal structural resolution of proteins through an information-theoretic analysis of their conformational ensemble,” *Journal of Chemical Theory and Computation*, vol. 22, pp. 1244–1257, 2026.
 - [30] J. Song, M. Marsili, and J. Jo, “Resolution and relevance trade-offs in deep learning,” *Journal of Statistical Mechanics: Theory and Experiment*, vol. 2018, p. 123406, 2018.
 - [31] R. J. Cubero, M. Marsili, and Y. Roudi, “Minimum description length codes are critical,” *Entropy*, vol. 20, p. 755, 2018.
 - [32] R. J. Cubero, J. Jo, M. Marsili, Y. Roudi, and J. Song, “Statistical criticality arises in most informative representations,” *Journal of Statistical Mechanics: Theory and Experiment*, vol. 2019, p. 063402, 2019.
 - [33] O. Duranthon, M. Marsili, and R. Xie, “Maximal relevance and optimal learning machines,” *Journal of Statistical Mechanics: Theory and Experiment*, vol. 2021, p. 033409, 2021.
 - [34] R. R. Sokal and C. D. Michener, “A statistical method for evaluating systematic relationships,” *University of Kansas Scientific Bulletin*, vol. 38, pp. 1409–1438, 1958.
 - [35] P. E. Smith, “The alanine dipeptide free energy surface in solution,” *The Journal of Chemical Physics*, vol. 111, pp. 5568–5579, 1999.
 - [36] L. Deng, “The mnist database of handwritten digit images for machine learning research [best of the web],” *IEEE Signal Processing Magazine*, vol. 29, pp. 141–142, 2012.
 - [37] P. G. Bolhuis, C. Dellago, and D. Chandler, “Reaction coordinates of biomolecular isomerization,” *Proceedings of the National Academy of Sciences*, vol. 97, pp. 5877–5882, 2000.